

PFC/JA-89-11

**Poloidal Field System Analysis
and Scenario Development for ITER**

Joel H. Schultz*
R. Bulmer[†] and J. Miller[†]

April 1989

**Plasma Fusion Center
Massachusetts Institute of Technology**

*** M.I.T. Plasma Fusion Center**

[†]Lawrence Livermore Laboratory

Submitted to *Nuclear Fusion*

I. INTRODUCTION

ITER, the International Thermonuclear Experimental Reactor, is a collaborative design by the United States, Europe, Japan and the Soviet Union of a tokamak fusion reactor that would demonstrate the physics and test the technology needed for commercial fusion reactors. The poloidal field (PF) magnets are responsible for forming and shaping highly elongated, high current plasmas, during a long-pulse burn. At least two classes of experiments must be supported by the PF system design, including inductively-driven, long-pulse burning discharges and discharges with steady-state current drive.

The PF coils are superconducting, using high performance, wind and react Nb_3Sn superconductor. The conductor/winding pack topology is a potted, internally-cooled cabled superconductor in a conduit (ICCS), circulating supercritical helium. The field and pulsed loss requirements are higher for the PF system than for the toroidal field (TF) system, although the steady-state heat removal requirement is not as high. The PF coils are designed up to maximum fields of 13.2 T and allowable field-current density products of 500 MAT/m². The field limits are reached at the beginning of initiation and the end of burn or beginning of shutdown in a typical scenario. In a scenario with rf-assisted start-up, limits may be reached at the end of start-up or the beginning of burn.

II. PULSED INDUCTIVE OPERATION

A. PF Scenarios

Poloidal field scenarios have been developed for several options. This report concentrates on the ohmic start-up and burn scenario for a 20 MA plasma. In this scenario, 240 V-s are used to bring the plasma to the beginning of burn, including an inductive requirement of 168 V-s and an average of 1 V resistive during start-up and auxiliary heating. The plasma can then be sustained for an additional 50 V-s. The scenario satisfies the physics and engineering constraints described in Table I. The PF currents also provide high-beta MHD equilibria at the beginning and end of burn and a broad field null at the beginning of initiation. The PF coil set is described in Table II.

The contributions of the various PF coils to the plasma volt-seconds are shown in Fig. 1. Over half of the volt-seconds needed for ignition are provided by PF5 and PF6, the vertical field coils. The loop voltage provided to the plasma for initiation is 15 V for 50 ms, which is aggressive in comparison with the designs of tokamaks not using any rf assist. However, there are large amounts of rf power available for initiation assistance, if needed.

The twelve poloidal field coils are driven by six symmetric power supplies. Peak currents and voltages in the PF coils have been held below 46 kA and 20 kV, respectively. The peak current and voltage are both on PF5, the upper outside vertical field coil. The PF5 negative current supply requires 45 kA and 6000 V, which requires seriesing of four rectifier bridges. This voltage is still within the capability of present-day rectifiers, without requiring enclosure in special insulating environments.

B. Method

A new PF trades code was developed to explore the limitations of a superconducting coil system with no constraints on plasma volt-second requirements. This permits the sizing of a broad range of experiments from full ohmic to full steady-state current drive. After the survey established a set of design allowables, the flux bias and volt-second swing were varied and compared with the abovementioned allowables. This analysis showed limits not

only on poloidal field flux at the beginning of initiation and at the end of burn, but also at the beginning of burn and the beginning of shutdown. This limit wasn't located at the equator of the central solenoid, but at its tips in the divertor region. The current design is somewhat unusual in that PF5 is also a limiting coil, having the highest JB product at the end of start-up. PF5 also has the highest tensile stress of any of the PF coils. Since PF5 is not restricted in allowable space, these limits could be eliminated by increasing PF5's cross section.

III. TIME HISTORY

A time scenario of the coil currents was developed that satisfied the magnet and physics constraints for the ohmic start-up and burn of a 20 MA plasma. The currents selected produce a scenario that reaches allowable limits at two points in time: preinitiation and beginning of shutdown. The characteristic double peak in B_{max} is seen in Fig. 2. The peak field, while generally in the ohmic solenoid stack is not necessarily at the equator, but moves up then down the stack during plasma start-up. At the end of start-up, the highest fields are in PF4, the divertor coil, and PF5. At the beginning of burn, when the divertor coil currents are highest, the peak field limitation is in PF4. The peak field appears at the equator of the central solenoid shortly into the burn period and remains there for the rest of the discharge. A similar pattern is shown in the constraint on JB_{max} . Stress limits are much more complex, because of the constraints on fatigue life, the complex load path in the ITER central solenoid stack, and constraints on local compression in the Nb₃Sn superconductor.

The minimum fraction of critical current within each coil was also calculated as a function of time. All coils use a square conductor with a conduit width of 3.83 cm. The equation for critical current was derived from the TIBER Final Design Report [HE85], being Miller's interpretation of Suenaga's data on MF-Nb₃Sn conductor with titanium additions [SU85]. The equation for critical temperature was derived from the measurements of Hudson, Yin and Jones [HU82]. The highest fraction of conductor critical current in the 20 MA scenario is 0.3 in PF3 towards the top of the central solenoid, at the beginning of plasma initiation. The highest fraction of conductor critical current after a current-conserving disruption is 0.4 in PF1 at the beginning of shutdown.

Another design requirement is that the energy margin should be greater than 500 mJ/cm³ at all times during scenario. The assumption made in this analysis is that deposition of energy into the metal is isothermal with respect to local helium in the conduit and adiabatic with respect to the inlet and outlet. The energy margin at all layers of each coil is calculated at each point in time for constant helium mass density. The minimum energy margin is 820 mJ/cm³ in PF1 at the beginning of initiation and again at the beginning of plasma shutdown, as shown in Fig. 3.

A. Power and Energy Requirements

The power and energy required from external power supplies are shown in Fig. 4. The power requirements are modest, compared with a much smaller next-step ignition experiment, such as CIT, because of the longer ramp times and the absence of resistive losses in the superconductors. The peak energy requirement is 13.7 GJ at the end of start-up and again at the beginning of shutdown. The dominant coil is PF5, the upper of the two outside ring coils which provides most of the vertical field at the end of start-up. The

upper ring coil has greater requirements than the lower throughout most of the scenario. This is the reverse of the situation in most PF scenarios and is a function of the specific MHD equilibria. The maximum positive power of 706 MW must be provided by a utility or local generator. The peak negative power of -1030 MW during initiation can be dumped in external resistors. As with the energy, line power is dominated by PF5, the upper ring coil, while the negative power at initiation is dominated by the central solenoid stack (PF1-3).

B. Load History

The hoop and vertical loads on each coil were calculated at each point in time. The average Tresca membrane stress in the conductor conduit was calculated at each point in time. The total load on each coil has been calculated following either current-conserving or flux-conserving disruptions, occurring at any time during the scenario. Even if all coils were entirely self-supporting, all coils would be within the static membrane allowable ($2/3$ yield stress of JBK-75 in the conduit), before and after disruption. The highest Tresca membrane stress in a self-supporting conduit for the reference scenario is 504 MPa at the bottom of the OH stack (PF1, PF2, PF3), as shown in Fig. 5. If the axial loads in PF1-3 could be decoupled, the highest Tresca membrane stress would be 482 MPa in PF3. The static allowable Tresca membrane stress is 800 MPa and the cyclic loading allowable for the reference scenario is 600 MPa. The hoop tension stress of 296 MPa could be greatly reduced by compression from the TF coils, as in the TIBER design [LE87]. Currently, ITER is considering a self-supporting central solenoid, so that tensile fatigue of the conduit will probably control the magnet structural design.

C. Pulsed Losses

Pulsed losses in the PF system have several large components. Losses in the PF windings are caused by superconducting hysteresis and transverse coupling. Pulsed losses in the cases are considered for transverse field pulses and induced electric fields. If there are no insulating breaks in the cases, the losses under a normal scenario due to parallel electric fields will be about six times higher than those due to pulsed magnetic fields.

The pulsed losses in the PF winding packs and cases during a normal scenario have been calculated. Losses in the winding packs and cases are shown in Fig. 6. The total system loss is 19 MJ, and every coil makes a significant contribution to the total. Nearly half of the losses are deposited during shutdown. The total loss in the cases is only 3.4 MJ, with losses in the central solenoid dominant. These could be reduced by further reducing the case thicknesses, since the windings are structurally self-supporting. For an 800 second overall cycle time, which would give a 50% local duty factor, the cryogenic refrigeration plant for the poloidal field system would be rated at 24 kW.

The losses in a disruption have been calculated by two methods, assuming that each PF coil conserves either current or flux. The accumulated losses before and after disruption for either assumption are calculated at every point in time for the PF winding packs, as shown in Fig. 7. The worst time for a disruption for either the current-conserving or the flux-conserving model is at the beginning of shutdown. If a current-conserving disruption occurred at the beginning of shutdown, a total of 18.5 MJ would be deposited in the winding packs. A flux-conserving disruption, which is closer to expected system behavior, can never deposit more energy than a normal discharge, because the coil losses are dominated by hysteresis. However, a flux conserving disruption at either end of start-up or beginning of

shutdown would deposit 17 MJ in the cases, as contrasted with the 3.5 MJ deposited in a normal discharge.

IV. OUT-OF-PLANE LOADS

The poloidal field system also creates out-of-plane overturning moments on the toroidal field (TF) magnets. A new code was developed in order to determine the times at which these loads are the most severe and also in order to evaluate the out-of-plane loads due to vertical disruptions. As shown in Fig. 8, the most severe out-of-plane loads occur at the end of start-up and the beginning of shutdown, at high current and low-beta, rather than at the high-beta end of burn, as is commonly assumed. A design rule that has recently been adopted for design against vertical disruptions specifies that the magnet systems must be able to withstand a full current plasma that is vertically displaced by half the vacuum vessel half-height. The running loads were calculated on the TF coils for plasmas displaced in either the upwards or downwards directions. The torque of the TF magnet system about the vertical axis was negligibly affected by such disruptions. However, Fig. 9 shows that the largest effect occurs on the net moment about the equator of each individual TF coil. The peak moment during a normal scenario occurs during the flat-top. A vertical disruption can increase the peak by 35% and a disruption at the beginning of shutdown can reverse the moment to 50% of the peak.

V. CONCLUSIONS

- Scenarios have been developed for a variety of ITER options, satisfying a broad range of physics and engineering constraints.
- The ITER PF system is capable of achieving the machine mission of creating a 20 MA ignited or heated plasma with a current flat-top of hundreds of seconds.
- With the current conductor design and self-supporting PF coils, the structural limits of the conduit are more constraining than the critical current and energy margin of the superconductor.
- The out-of-plane loads on the TF magnets are dominated by high-current, low-beta plasmas and the response to vertical disruptions.

References

- [HE85] C.D. Henning and B.G. Logan et al., 'TIBER Final Design Report,' LLL UCID-20589, Nov 1985.
- [HU82] P.A. Hudson, F.C. Yin, and H. Jones, 'The critical current density of filamentary Nb₃Sn as a function of temperature and magnetic field,' IEEE Trans. Mag., MAG-19, No.3, pp 903-906, 1983.
- [LE87] J.D. Lee, ed., 'TIBER II/ETR Final Design Report,' UCID-21150, Sept 1987.
- [SU85] M. Suenaga, DOE Workshop on Conductor-Sheath Issues for ICCS, Germantown, MD, July 15-16, 1985.

Table I
Poloidal Field System Constraints

I_p	20	(MA)
$V\text{-}S_{swing,EOB}$	290	(V-s)
V_{init}	15	(V)
B_{max}	13.2	(T)
JB_{max}	500	MA-T/m ²
$\sigma_{Trescamembrane}$	600	(MPa)
$V_{terminal}$	20	(kV)
I_{cond}	45	(kA)

Table II
ITER PF System Winding Pack Dimension

Coil	R (m)	Z (m)	R ₁ (m)	R ₂ (m)	Z ₁ (m)	Z ₂ (m)	n _{turns}
PF1,U,L	1.7	± 1.5	1.4	2.0	± 0.0	± 3.0	1095
PF2,U,L	1.7	± 4.0	1.4	2.0	± 3.0	± 5.0	730
PF3,U,L	1.7	± 6.5	1.4	2.0	± 5.0	± 8.0	1095
PF4,U,L	4.0	± 8.2	3.5	4.5	± 7.7	± 8.7	608
PF5,U,L	11.5	± 6.0	11.25	11.75	± 5.5	± 6.5	304
PF6,U,L	11.5	± 3.0	11.25	11.75	± 2.5	± 3.5	304

Plasma Volt-Seconds (Wb) vs. Time (s)

ITER

VS,max (Wb) = 111.879

Vs,min (Wb) = -177.533

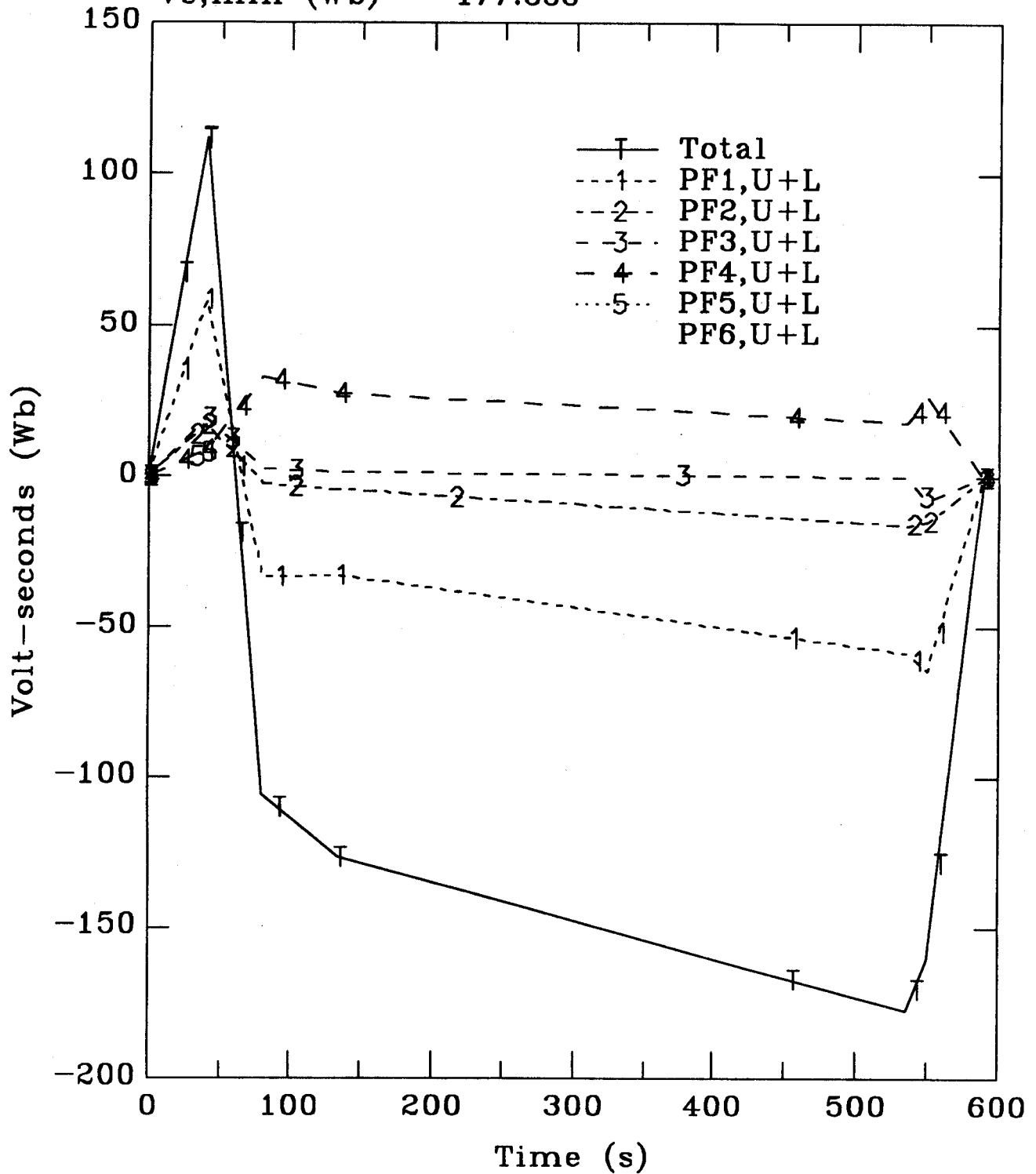


Figure 1
PF Coil contributions to Plasma Volt-Seconds

Maximum Flux Densities (T) vs. Time (s) ITER

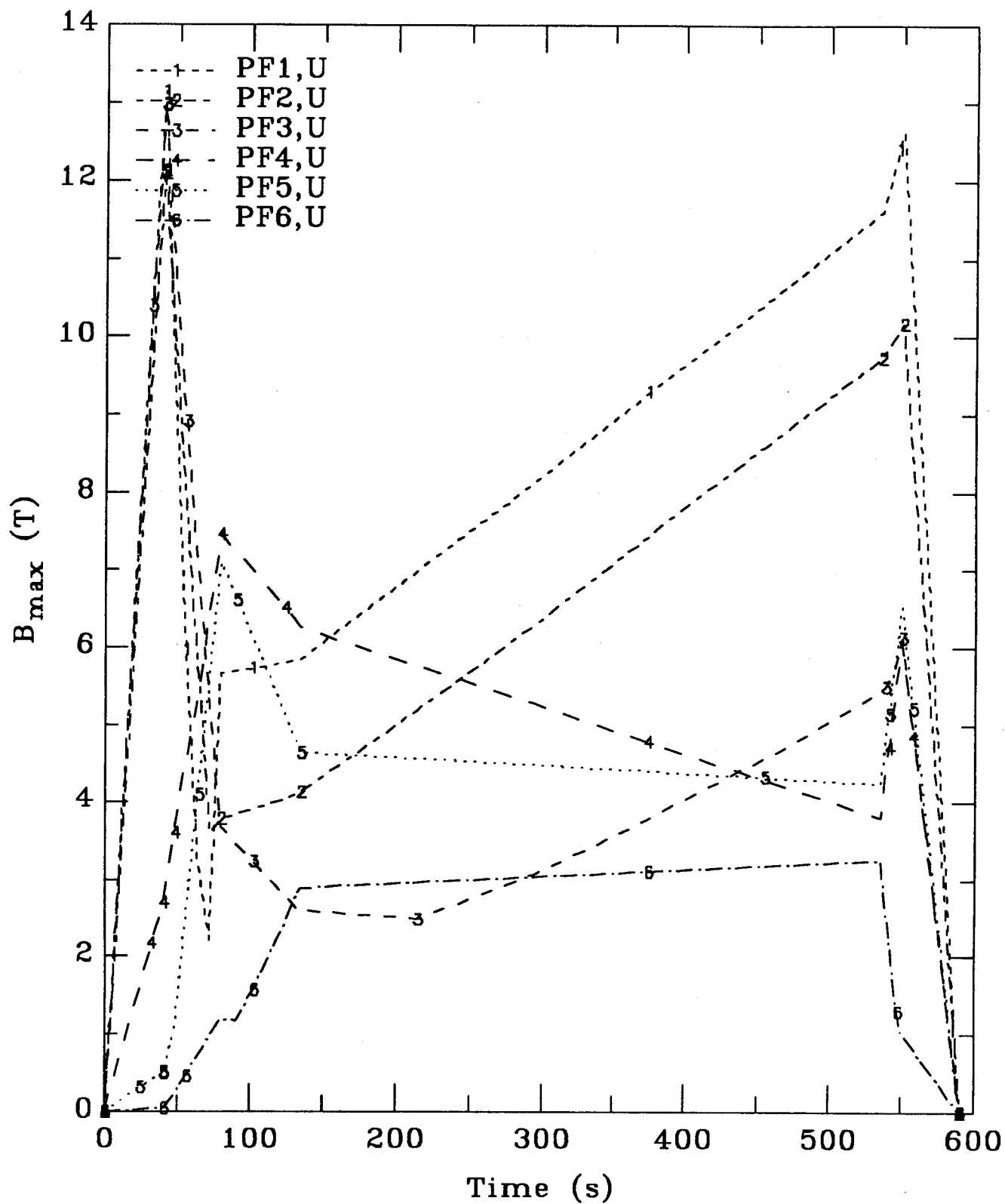


Figure 2
Maximum Field in Pf Coils (T) vs. Time (s)

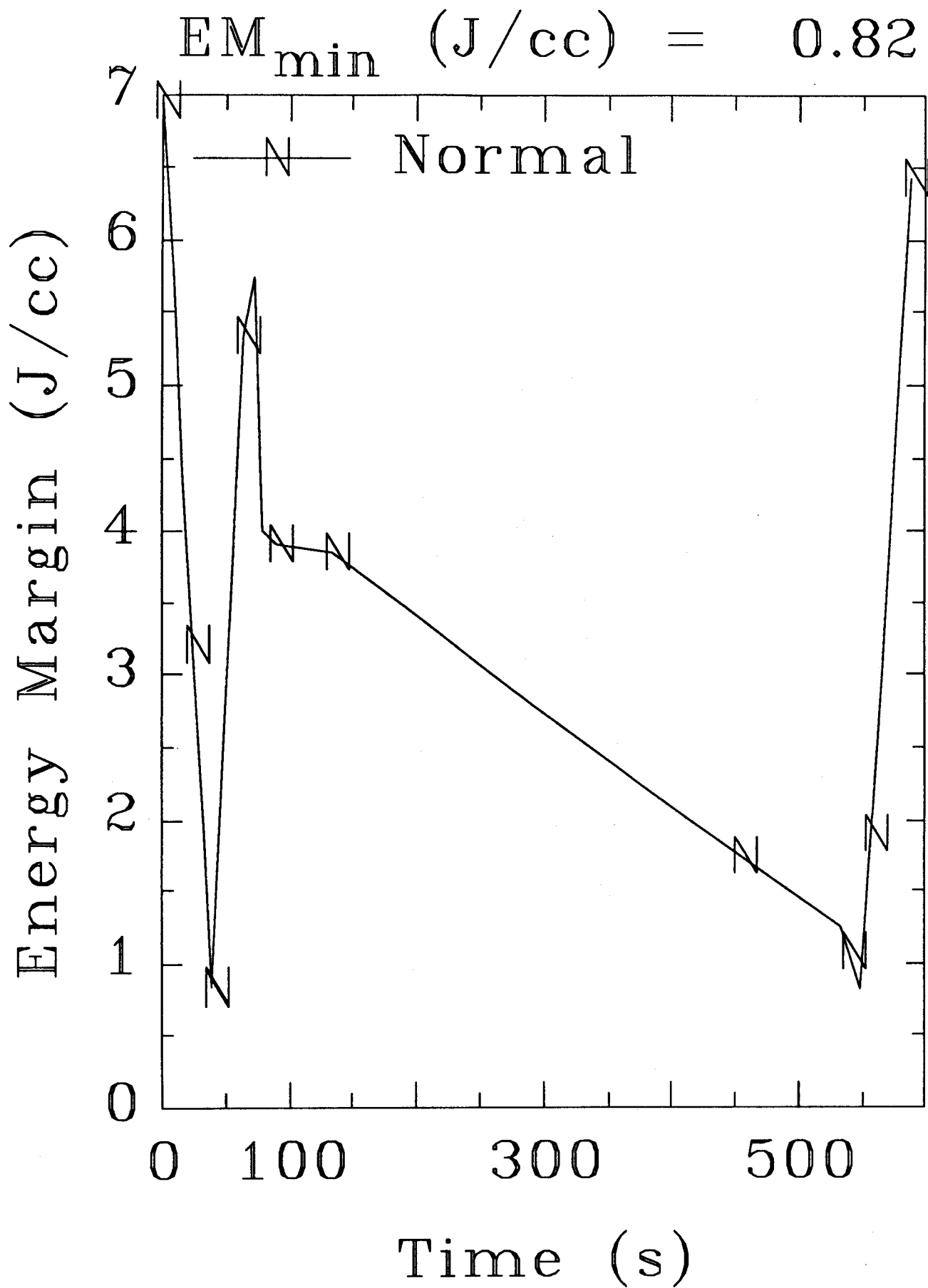


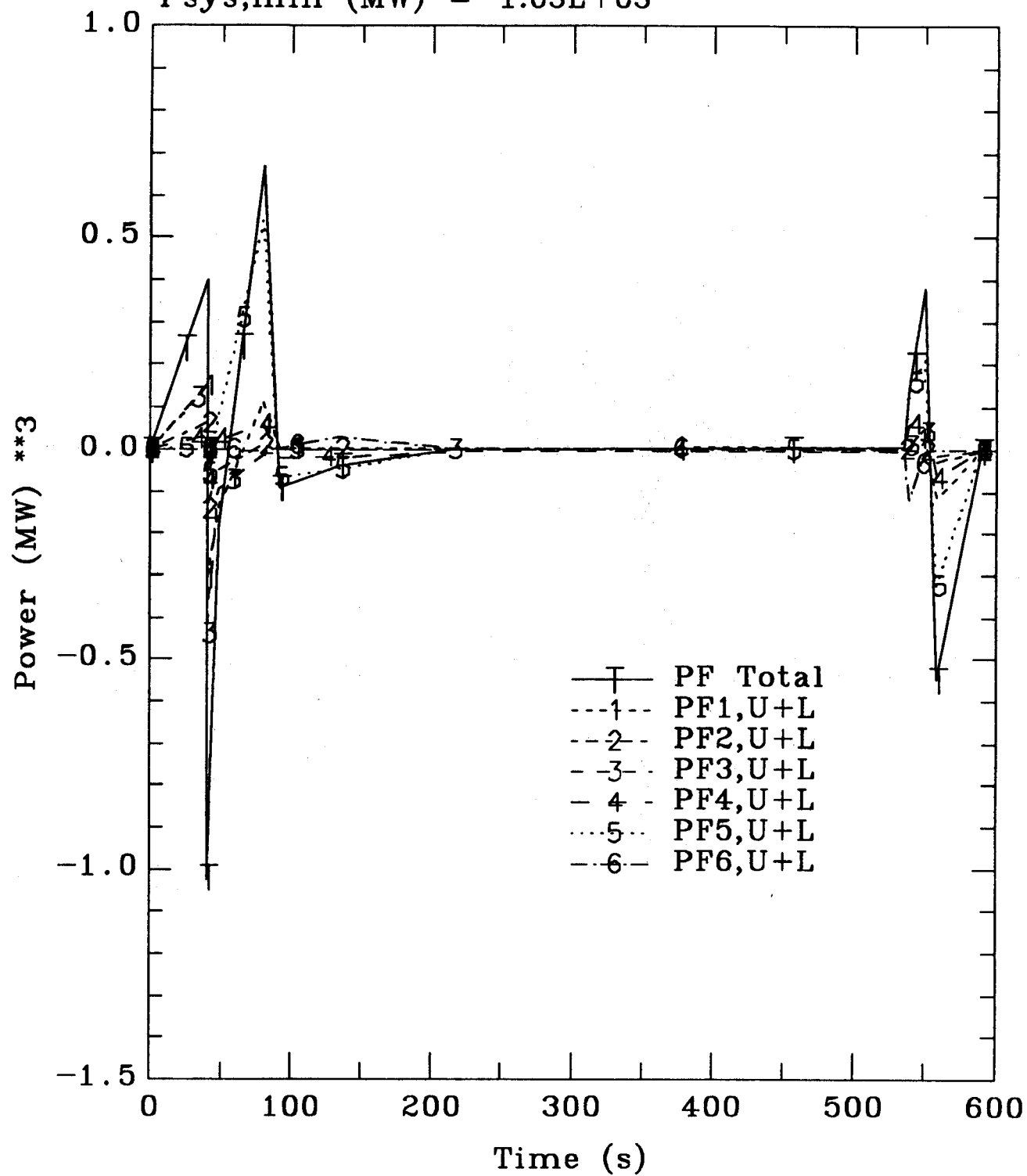
Figure 3
Minimum Energy Margin (mJ/cc), PF1

PF System Power Flow (MW) vs. Time (s)

ITER

Psys,max (MW) = 706.076

Psys,min (MW) = -1.03E+03



4.a

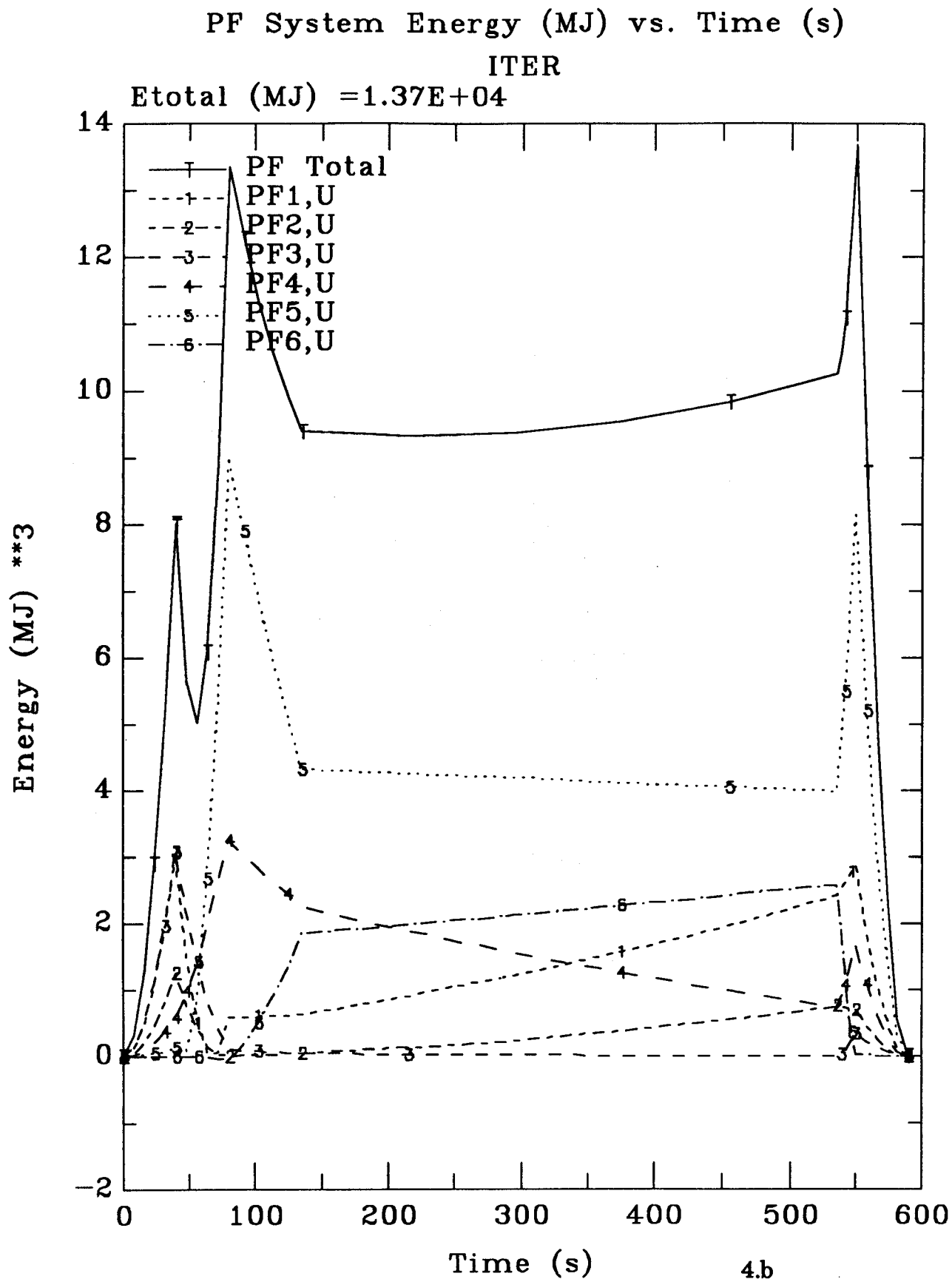


Figure 4.a,b
ITER Power and Energy Requirements

OH,U Tresca Membrane Stress in conduit
Tensile Stress (MN) vs. Time (s)
 R_c (m) = 1.700 Z_c (m) = 1.500
 dR (m) = 0.600 dZ (m) = 3.000
 σ_{Tmax} (MPa) = 295.56
 σ_{Tmin} (MPa) = 0.00

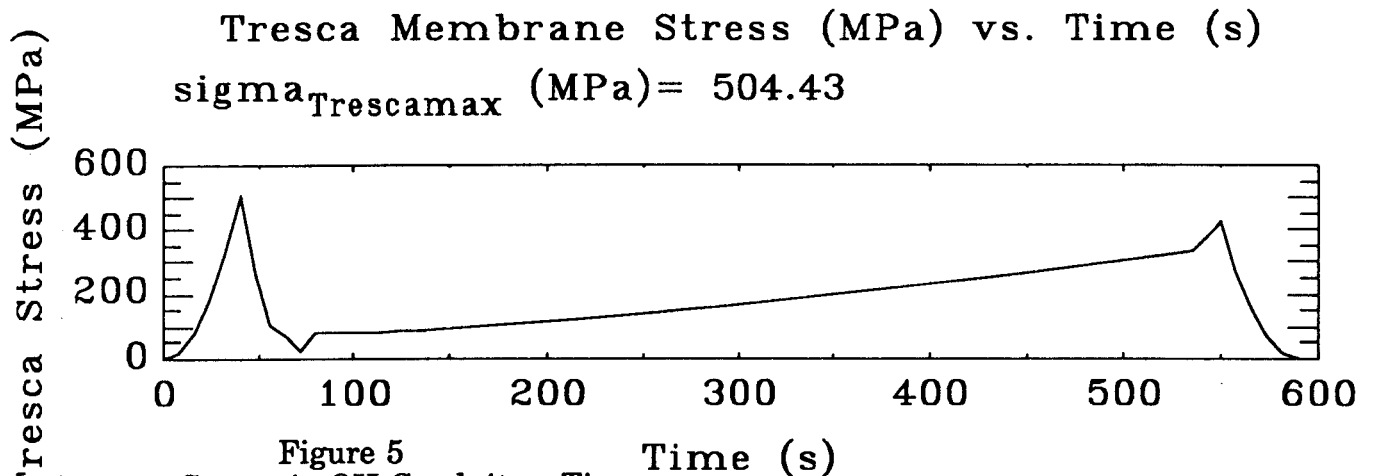
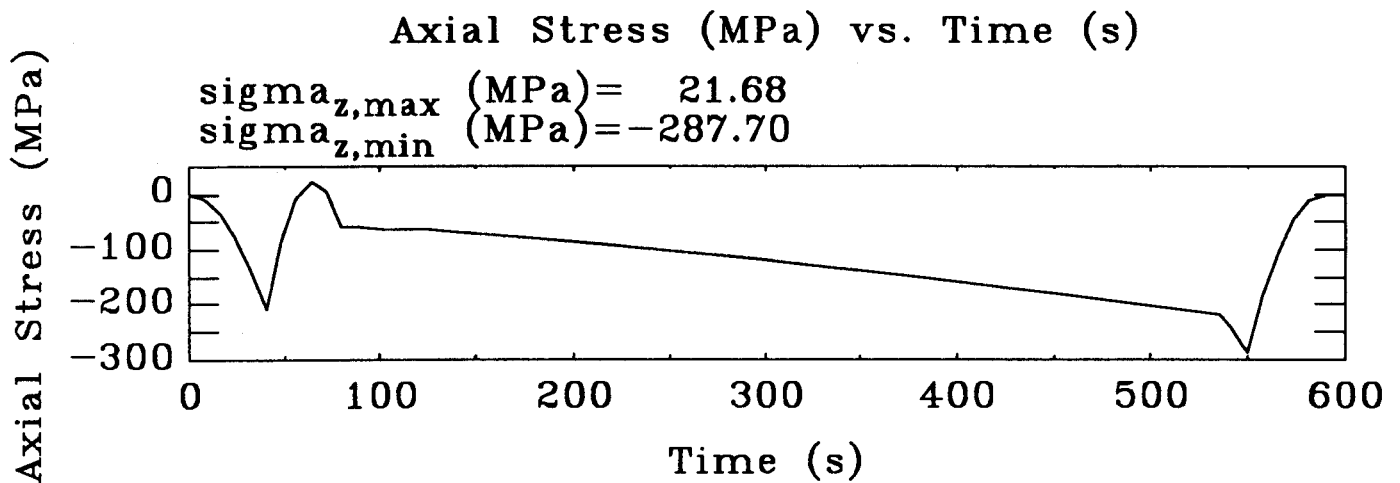
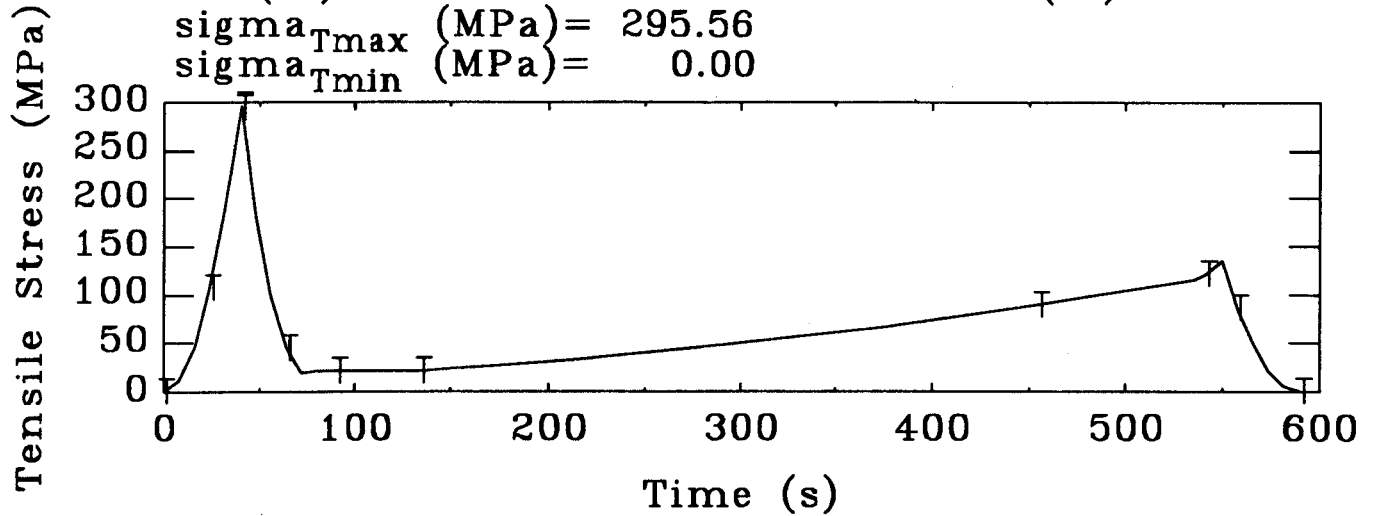
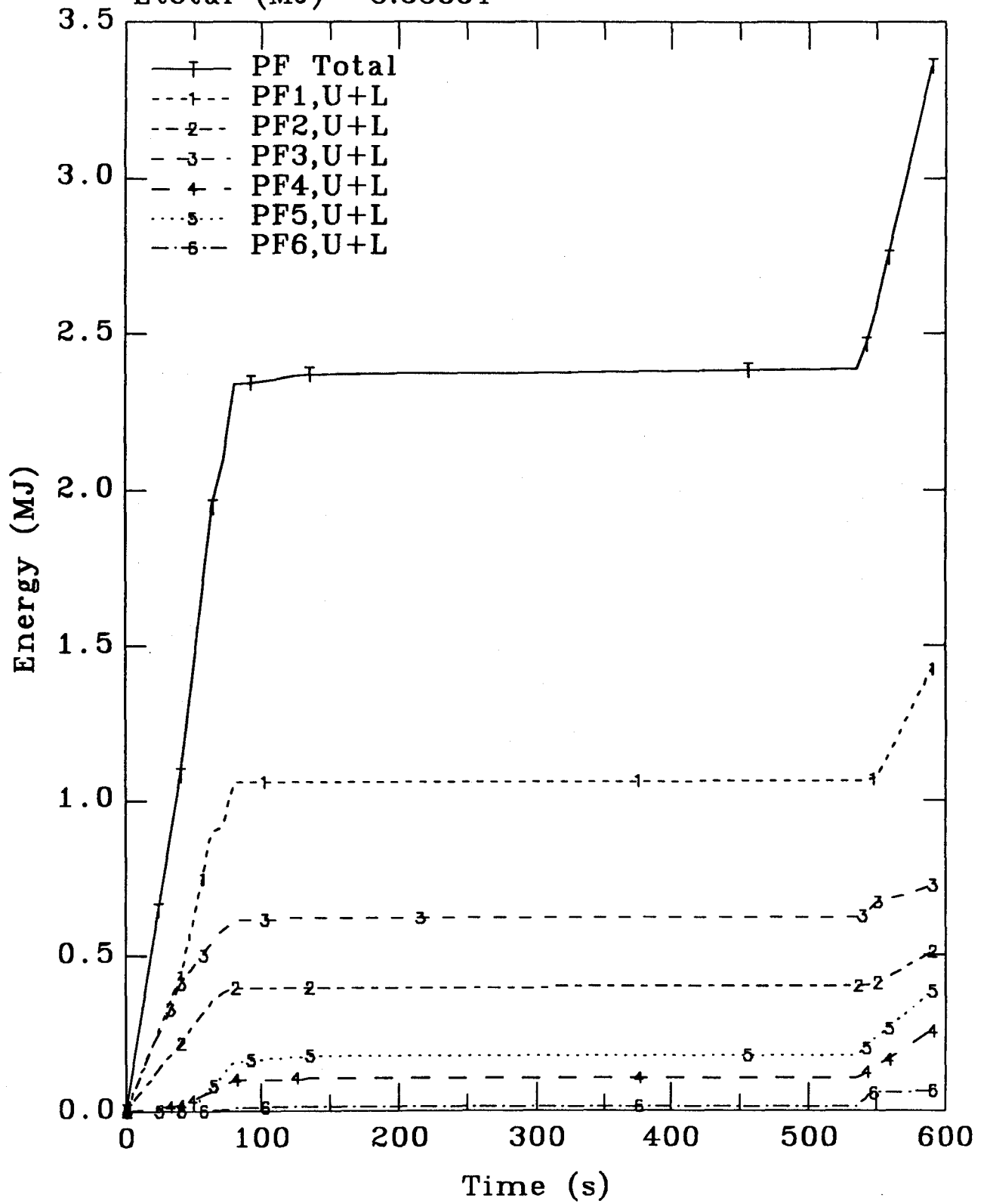


Figure 5
Average Stress in OH Conduit vs Time

Losses in PF Cases (MJ) vs. Time (s)

ITER

$E_{total} \text{ (MJ)} = 3.35864$



6.a

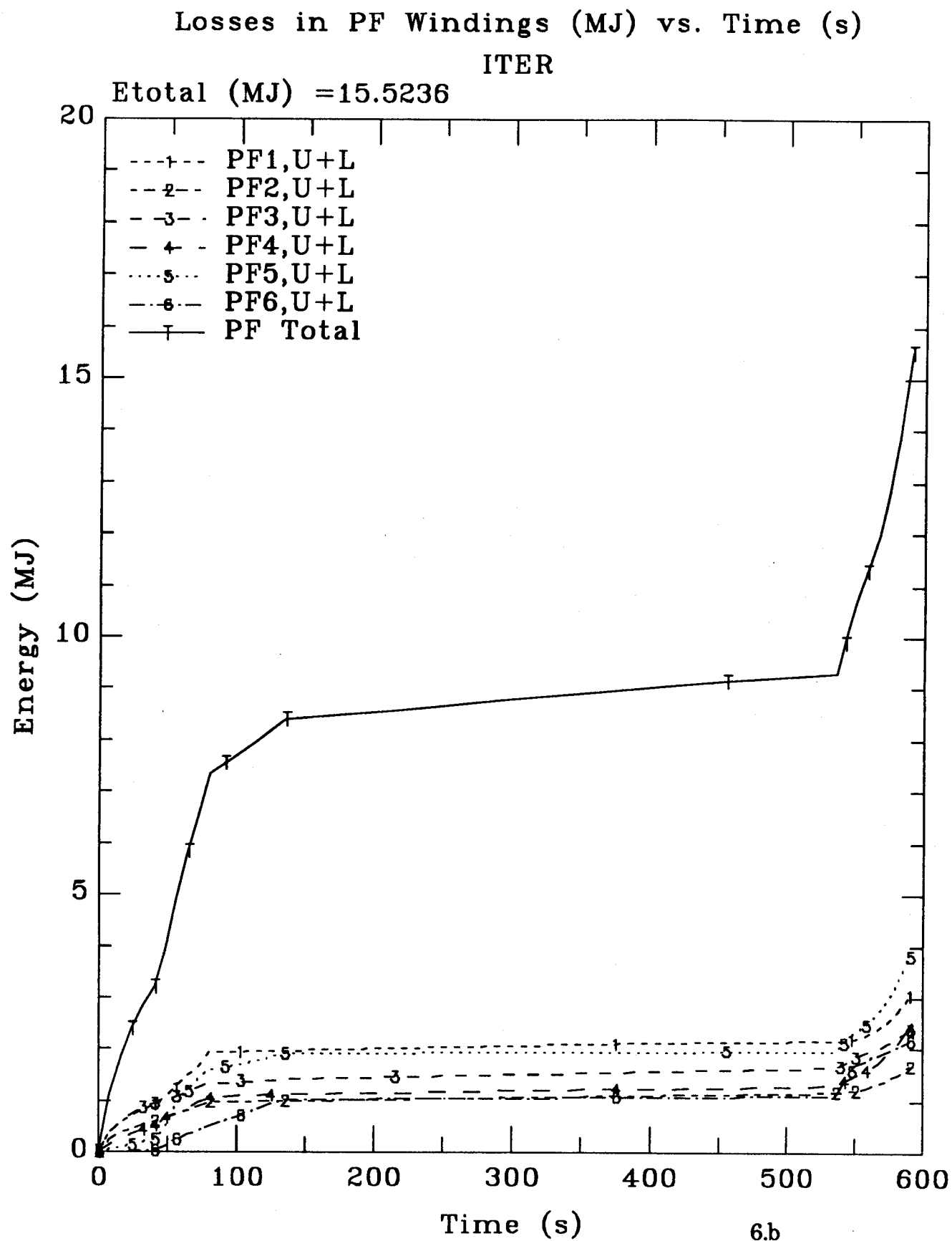


Figure 6.a,b
Pulsed Losses in PF Winding Packs and Cases

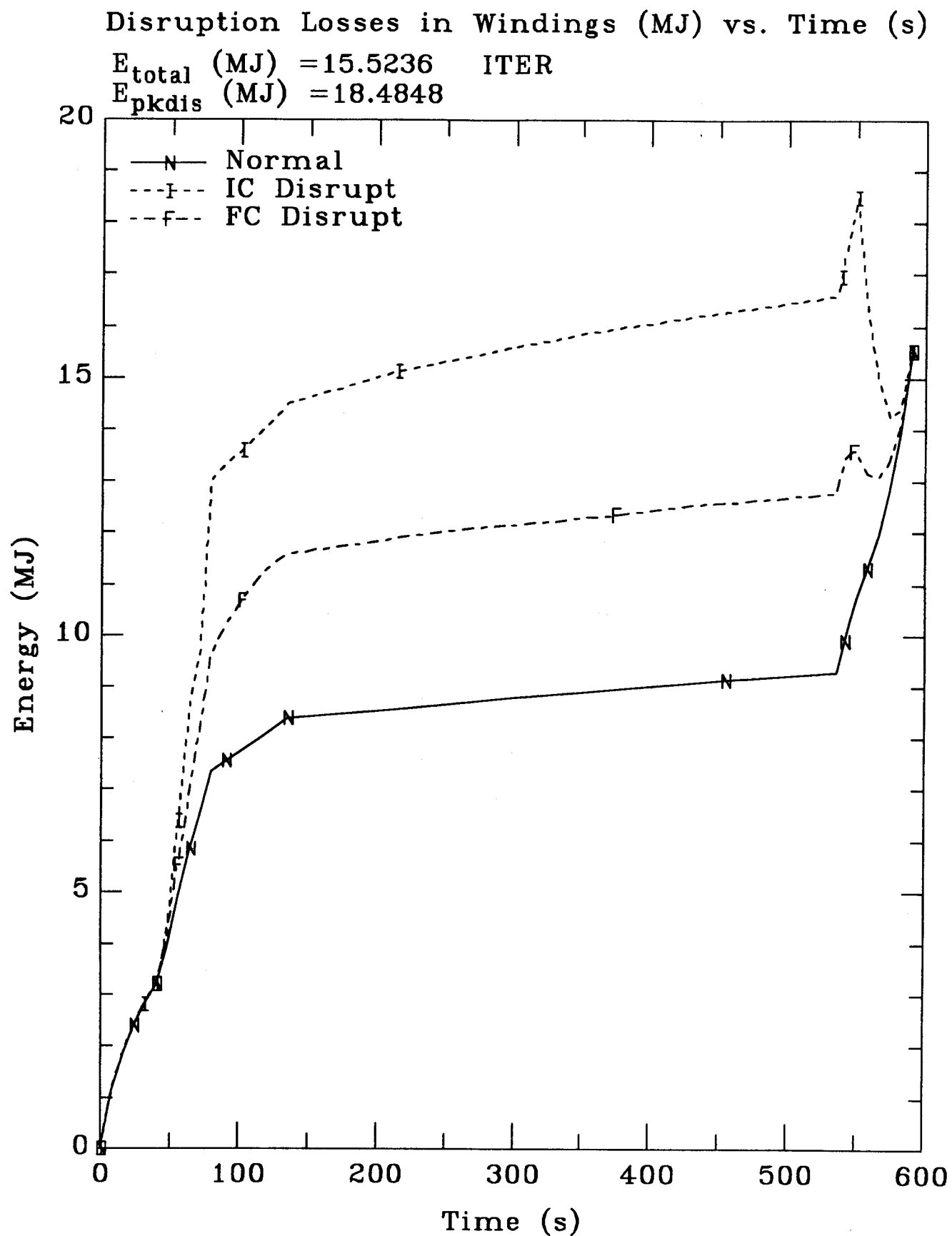


Figure 7
Disruption Losses (MJ) in PF Winding Packs

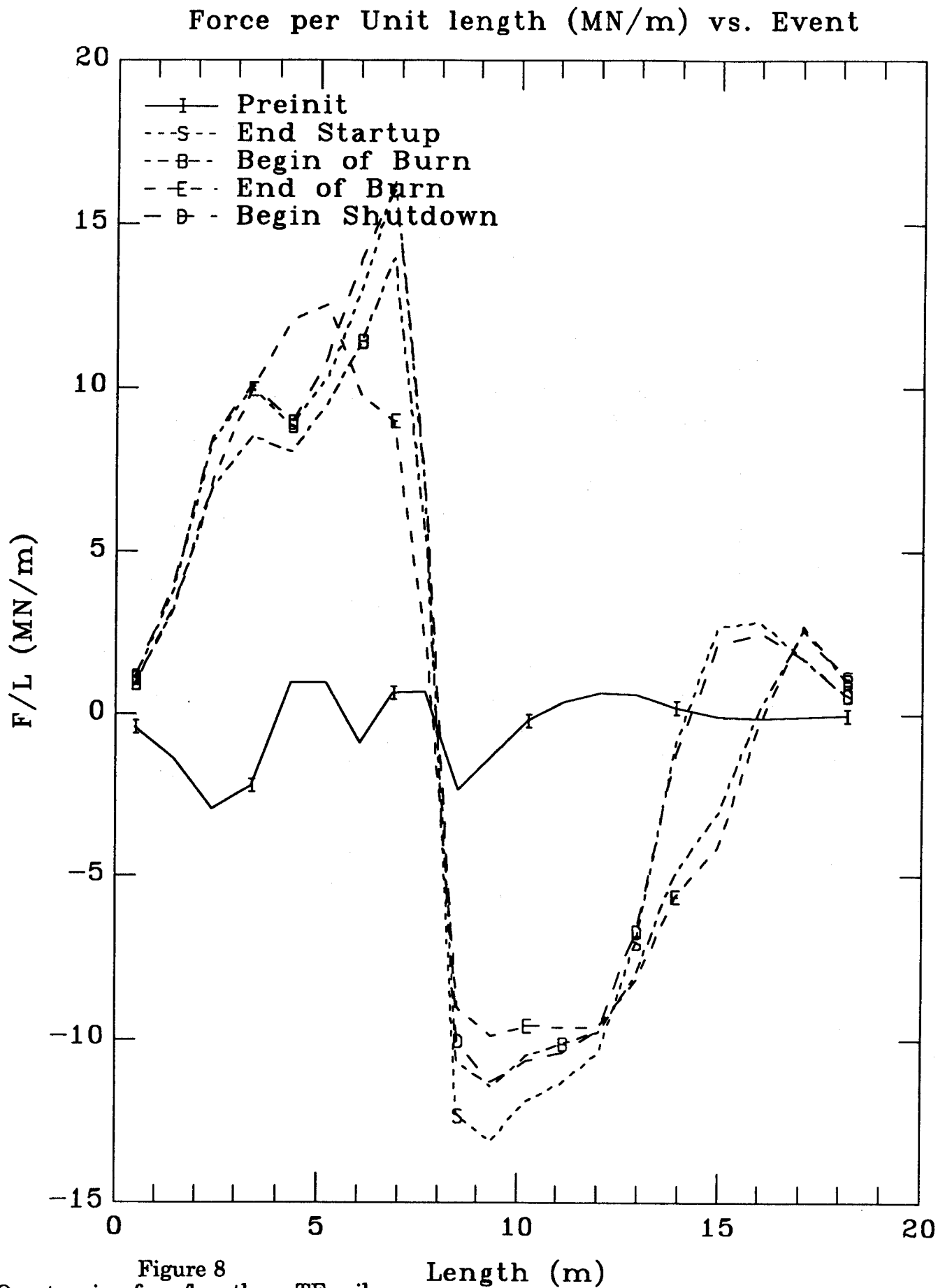


Figure 8
Overturning force/length on TF coil

Moment about equator, 1 coil (MN-m) vs. Time (s)

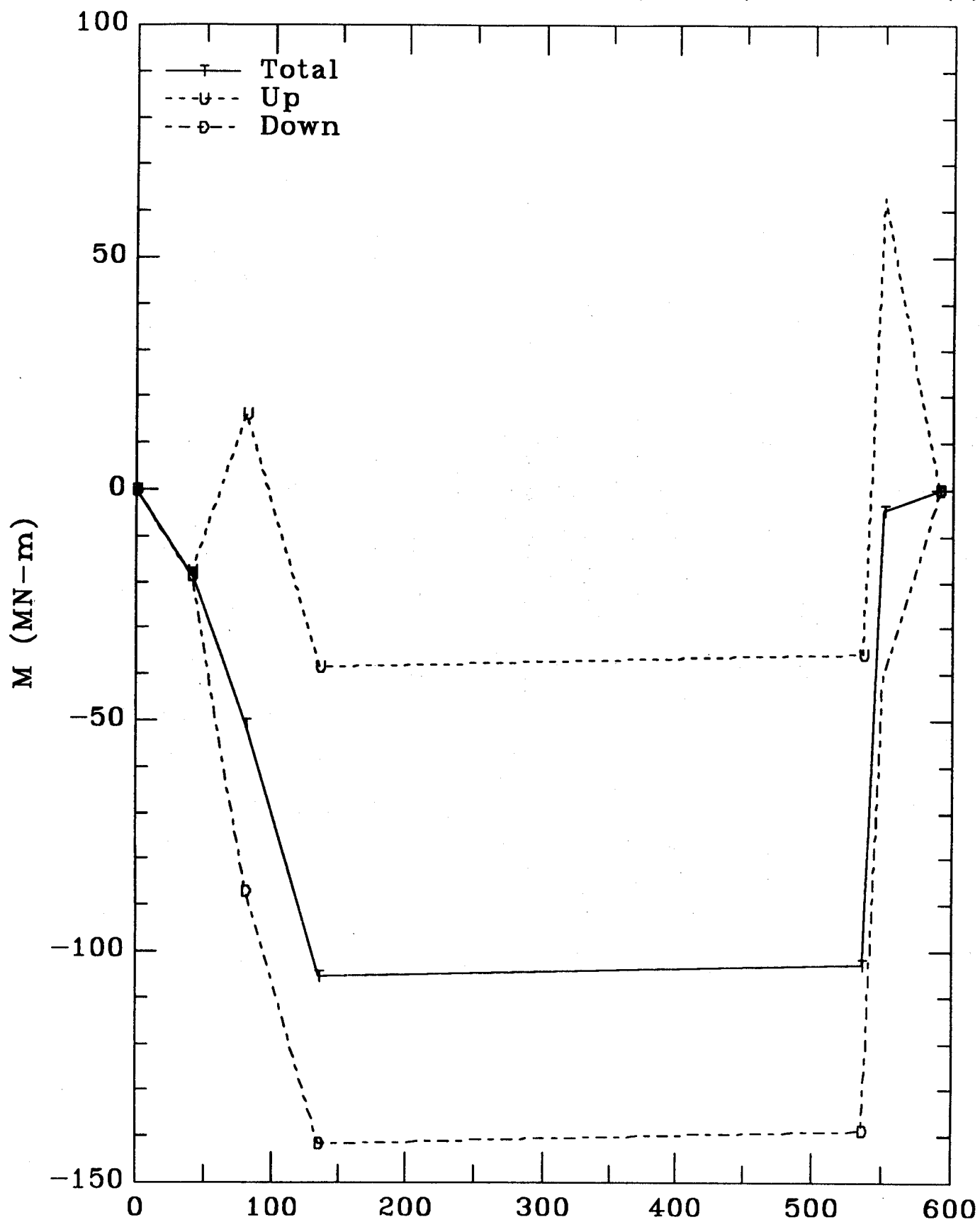


Figure 9
Overturning moment, normal+disruptions